

Music Boundary Detection using Convolutional Neural Networks: A comparative analysis of combined input features

Carlos Hernandez-Olivan, Jose R. Beltran, David Diaz-Guerra

Abstract—The analysis of the structure of musical pieces is a task that remains a challenge for Artificial Intelligence, especially in the field of Deep Learning. It requires prior identification of structural boundaries of the music pieces. This structural boundary analysis has recently been studied with unsupervised methods and *end-to-end* techniques such as Convolutional Neural Networks (CNN) using Mel-Scaled Log-magnitude Spectrograms features (MLS), Self-Similarity Matrices (SSM) or Self-Similarity Lag Matrices (SSLM) as inputs and trained with human annotations. Several studies have been published divided into unsupervised and *end-to-end* methods in which pre-processing is done in different ways, using different distance metrics and audio characteristics, so a generalized pre-processing method to compute model inputs is missing. The objective of this work is to establish a general method of pre-processing these inputs by comparing the inputs calculated from different pooling strategies, distance metrics and audio characteristics, also taking into account the computing time to obtain them. We also establish the most effective combination of inputs to be delivered to the CNN in order to establish the most efficient way to extract the limits of the structure of the music pieces. With an adequate combination of input matrices and pooling strategies we obtain a measurement accuracy F_1 of 0.411 that outperforms the current one obtained under the same conditions.

I. INTRODUCTION

Music Information Retrieval (MIR¹) is the interdisciplinary science for retrieving information from music. MIR is a field of research that faces different tasks in automatic music analysis, such as pitch tracking, chord estimation, score alignment or music structure detection.

This paper deals with the issue of structure detection in musical pieces. In particular, the comparison of different methods of boundary detection between the musical parts by means of Convolutional Neural Networks has been addressed.

One of the most active and one of the scientific reference in MIR is the Music Information Retrieval Evaluation eXchange (MIREX²). This is a community which every year holds the International Society for Music Information Retrieval Conference (ISMIR). Algorithms are submitted to be tested in MIREX's datasets within the different MIR tasks. Most of the previous results analyzed and compared in this work have been presented in different MIREX campaigns.

Musical analysis [1], viewed from the point of music theory, is a discipline which studies the musical structure in order to get a general and thorough comprehension of the music. It is a very complex task in music theory because the analysis of musical pieces from the same period or from different periods

in the history of music can be carried out in many different ways. The concept of musical analysis has evolved throughout history and has included different types of analysis, such as formal analysis, harmonic analysis, and stylistic analysis. In this work we will study the formal analysis, in other words, the structural analysis of musical pieces.

The automatic structural analysis of music is a very complex challenge that has been studied in recent years, but it has not yet been solved with an adequate quality that surpasses the analysis performed by musicians or specialists. This kind of analysis is only a part of the musical analysis that involves musical aspects like [2] harmony, timbre and tempo, and segmentation principles like repetition, homogeneity and novelty. The benefits of solving this task comes from the importance of understanding how music is formed; the narrative, performing, the particularities in the techniques of composing of an author or period, in other words, the pillars of music composition. This automatic music analysis can be faced starting from music representations such as the score of the piece, the MIDI file or the raw audio file.

In music, *form* refers to the structure of a musical piece which consist on dividing music in small units starting with motifs, then phrases and finally sections which express a musical idea. *Boundary detection* is the first step that has to be done in musical form analysis which must be done before the naming of the different segments depending on the similarity between them. This last step is named *Labelling* or *Clustering*. This task, translated to the most common genre in MIREX datasets, the pop genre, would be the detection and extraction of the chorus, verse or introduction of the corresponding song. Detecting the boundaries of music pieces consists on identifying the transitions where these parts begin and end, a task that professional musicians do almost automatically by seeing a score. This detection of the boundaries in a musical piece is based on the *Audio Onset Detection* task, which is the first step for several higher-level music analysis tasks such as beat detection, tempo estimation and transcription.

The automatic analysis of musical forms studies the *musical form* by segmenting music signals. It is important to say that there is not a rule or a defined method to analyze music, so, even though the most typical musical forms like the Sonata, the Minuet and other musical forms have their respective structure, there is a lot of music that can be analyzed in different ways.

As mentioned above, after identifying the limits of a piece of music, the labelling phase must be carried out. This phase is the main objective of the structural analysis of the music and, regardless of the way the analysis is performed (unsupervised or *supervised neural network* methods), the first step to be carried out is the boundary detection.

This problem can be accomplished with different techniques

C. Hernandez-Olivan, J.R. Beltran, and D. Diaz-Guerra are with the Department of Electronic Engineering and Communications, University of Zaragoza, Zaragoza, Spain

¹<https://musicinformationretrieval.com/index.html>

²https://www.music-ir.org/mirex/wiki/MIREX_HOME

that have in common the need of pre-processing the audio files in order to extract the desired audio features and then apply unsupervised or *supervised neural network* methods. There are several studies where this pre-processing step is made in different ways, so there is not yet a generalized input pre-processing method. The currently *supervised neural network* best-performing methods use CNNs trained with human annotations. The inputs to the CNN are Mel-Scaled Log-magnitude Spectrograms (MLSs) [3], Self-similarity Lag-Matrices (SSLMs) in combination with the MLSs [4] and also combining these matrices with chromas [5].

One of the limits of these methods is that the analysis and results obtained depend largely on the database annotator, so there could be inconsistencies between different annotators when analyzing the same piece. These methods are limited to the quality of the labels given by the annotators so they cannot outperform them.

The paper is structured as follows: Section 2 presents an overview of the related work and previous studies in which this work is based on. The Self-Similarity Matrices and the used datasets are also presented. In Section 3, the pre-processing method of the matrices which will be the inputs to the NN is explained. Section 4 introduces the database used for training, validating and testing, and the labelling process. Section 5 shows the NN structure and the thresholding and peak-picking strategies and section 6 describes the metrics used to test the model and exposes the results of the experiments and their comparison with previous studies. Finally, section 7 presents the conclusions and a proposal for future lines of work.

II. RELATED WORK

Several studies have been done in the field of structure recognition in music since Foote in 1999 introduced the self-similarity matrix [6] and later, in 2003 Goto derived from it the self-similarity lag matrix [7]. Before that, the studies were based on processing spectrograms [8], but in the recent years it has been demonstrated that SSM and SSLM calculated from audio features along with spectrograms perform better results.

A. Unsupervised Methods

It is difficult to make a difference between works which try to extract only the boundaries of music pieces and the ones which try to cluster the different parts of the structure of music, because the principal idea of unsupervised methods is to extract the musical structure of music pieces but not the boundaries, so we describe some previous work in both areas which belongs to the same task in MIREX's campaigns, Music Structure Segmentation task.

These methods can be summarized in three approaches, according to Paulus et al. [23], based on: novelty, homogeneity and repetition. These approaches are computed with unsupervised and supervised Machine Learning algorithms such as genetic algorithms (*fitness functions*), Hidden Markov Models (HMM), *K-means*, Linear Discriminant Analysis (NDA), Decision Stump or Checkerboard-like kernels.

Novelty-based approach consists on the detection of the transitions between contrasting parts. This approach is well-performed using checkerboard-like kernel methods. These methods are based on the construction of a 2D kernel which is applied to the similarity matrix in order to measure the self-similarity on either side of the center point of a similarity matrix. The value of the measure is high when both regions are self-similar. The measure of the *cross-similarity* between the two regions is then calculated. The difference between this two measures estimates the novelty of the signal at the center point. This was introduced by Foote in 2000 [24] who used this method to extract the segment boundaries of the audio tracks using the similarity matrix as input, and then calculating the correlations with the proper kernel. These methods have evolved over the years and it was found that multiple-temporal-scale kernels as Kaiser and Peeters did in 2013 [25]. In this case, a fusion of the novelty and repetition approaches is proposed.

Homogeneity-based approach is based on the identification of sections that are consistent with respect to their musical properties. These methods used Hidden Markov Models, like Logan and Chu did in 2000 [26], Aucouturier and Sandler in 2001 [27] or Levy and Schandler in 2008 [28]. Hidden Markov Models (HMM) are based on augmenting Markov chains and seek statistical models that reflects the structure of the data, so they can learn the segmentation of the music signal. These methods used as inputs audio feature vectors such as MFCCs, and later on, in 2019, self-similarity matrices in Traile and McFee work [29] where they combined different frame-level features such as MFCCs, chromas, chord estimation CREMA model [30] and tempograms by using a Similarity Network Fusion (SNF) to later compute the segmentation and clustering with the L-measure method.

Repetition-based approach refers to the determination of recurring patterns. These methods apply a clustering algorithm to the Self-Similarity or Self-Similarity Lag Matrices. They are more applicable for labeling the structural parts of music pieces than for precise segmentation as required by boundary detection. Lu et al. in 2004 [31], and Paulus and Klapuri in 2006 [32] are examples of this techniques. The segmentation with repetition approach was done by Turnbull et al. in 2007 [19] who combined temporally-local audio features in an approach of the AdaBoost algorithm with a Boosted Decision Stump (BDS). Later on, McFee and Ellis [13] in 2014 used a Linear Discriminant Analysis, the Fisher's linear discriminant, that simultaneously maximizes the distance between class centroids, and minimizes the variance of each class individually. In 2019, McCallum [33] used unsupervised training of deep feature embeddings using Convolutional Neural Networks (CNNs) for music segmentation. These techniques did not show significantly improve in the results with respect to the classic unsupervised algorithms that have been described previously.

To finish, we can affirm that unsupervised algorithms are very efficient performing the labelling (clustering) part, but not the boundaries detection task that are better performed by *supervised neural networks* which came up in 2014 and are described in the next section.

³[https://www.music-ir.org/mirex/wiki/\(\(year\)\):MIREX\(\(year\)\)_Results_headland "Music Structure Segmentation Results"](https://www.music-ir.org/mirex/wiki/((year)):MIREX((year))_Results_headland_Music_Structure_Segmentation_Results).

TABLE I: Results of boundary detection of previous studies for "Full Structure" and "Segmentation" tasks. It is only showed the best-performing algorithm of each year in terms of F-measure for a $\pm 0.5s$ time-window tolerance according to MIREX09 from 2009 to 2011 and SALAMI dataset for 2012 onwards. Superindex * denotes that the results have been extracted from MIREX's campaigns from year 2009 to 2017.

Unsupervised Methods								
Year ³	Autors [Ref.]	Algorithm	Input	Method	F-measure (F_1) for Testing Databases			
					MIREX09	RCW-A	RCW-B	SALAMI
2009	Paulus & Klapuri [9]	PK	MFCCs, chromas	<i>Fitness function</i>	0.27	-	-	-
2010	Mauch et al. [10]	MND1	MFCCs, Discrete Cepstrum	<i>HMM</i>	0.325	0.359	-	-
2011	Sargent et al. [11]	SBVRS1	Chords estimation	<i>Viterbi</i>	0.231	0.324	-	-
2012	Kaiser et al. [12]	KSP2	SSM	<i>Novelty measure</i>	0.280	0.366	0.289	0.286
2013	McFee & Ellis [13]	MP2	MLS	<i>Fisher's Linear Discriminant</i>	0.281	0.355	0.278	0.317
2014	Nieto & Bello [14]	NB1	MFCCs + chromas	<i>Checkerboard-like kernel</i>	0.289	0.352	0.269	0.299
2015	Cannam et al. [15]	CC1	Timbre-type histograms	<i>HMM</i>	0.197	0.224	0.203	0.213
2016	Nieto [16]	ON2	Constant-Q Transform Spectrogram	<i>Linear Discriminant Analysis</i>	0.259	0.381	0.255	0.299
2017	Cannam et al. [15]	CC1	Timbre-type histograms	<i>HMM</i>	0.201	0.228	0.192	0.212
Supervised Neural Networks								
2014	Schlter et al. [17]	SUG1	MLS	CNN	0.434	0.546	0.438	0.529
2015	Grill & Schlter [18]	GS1	MLS + SSLMs	CNN	0.523	0.697	0.506	0.541

TABLE II: Results of previous works in boundary detection task for $\pm 0.5s$ time-window tolerance. It is only showed the best F-measure result of each reference for each database.

Unsupervised Methods								
Year	Autors [Ref.]	Input	Method	Train Set	F-measure (F_1) for Testing Databases			
					MIREX09	RCW-A	RCW-B	SALAMI
2007	Turnbull et al. [19]	MFCCs, chromas, spectrogram	<i>Boosted Decision Stump</i>	-	-	-	0.378	-
2011	Sargent et al. [20]	MFCCs, chromas	<i>Viterbi</i>	-	-	-	0.356	-
Supervised Neural Networks								
2014	Ullrich et. al [21]	MLS	CNN	Private	-	-	-	0.465
2015	Grill & Schlter [4]	MLS + SSLMs	CNN	Private	-	-	-	0.523
2015	Grill & Schlter [5]	MLS + PCPs + SSLMs	CNN	Private	-	-	-	0.508
2017	Hadria & Peeters [22]	MLS + SSLMs	CNN	SALAMI	-	-	-	0.291

B. Supervised Neural Networks

The term *end-to-end learning* refers to the architectures that goes from a pre-processed input to the desired output [34]. These models learn from data so they can generalize much better than unsupervised methods and require less manual pre-processing. A general block diagram of this method is presented in Figure 1.

Previous studies used Mel-Scaled Log-magnitude Spectrograms (MLS) as the inputs of CNNs for boundaries detection [3]. This method was based on *Audio Onset Detection* MIREX task which consist on finding the starting points of all musically relevant events in an audio signal, in particular, in the algorithm presented in the 2013 MIREX campaign [21]. Onsets detection in audio signals consist on the detection of events in music signals, specifically the beginning of a music note. It can be interpreted as a computer vision problem, like edge detection, but applied to spectrograms instead of images

with different textures.

Later on, in 2015, Grill and Schulter improved their previous work by adding SSLMs to the input which yielded to better results [4] and the addition of SSLMs with different lag factors to the input of the CNN [5] outperformed this method giving the best result to date.

In Tables I and II a recap of the results of all the previous works done in boundaries detection for unsupervised and supervised neural networks are presented. Results and "Code" names in Table I have been extracted from MIREX's campaigns of different years. It must be said that the results obtained with unsupervised methods on Table I are not as high as the results obtained with supervised neural networks because their goal was not the boundary detection (segmentation) itself but the full structure identification (labelling).

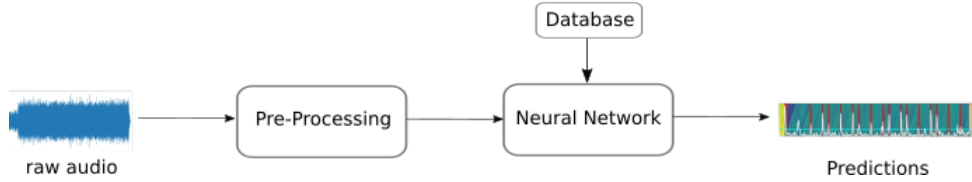


Fig. 1: General scheme of *supervised neural networks*.

C. Self-Similarity Matrices (SSM)

The Self-Similarity Matrix [2] is a tool not only used in music structure analysis but in time series analysis tasks. Its homogeneous regions representing the structural elements of music analysis leads this matrix and its combination with spectrograms to be the input of almost every model described in sections II-A and II-B. In this work, this matrix is important because music is in itself *self-similar*, that is, it is formed by similar time series.

Self-Similarity Matrices have been employed under the name of Recurrence Plot for the analysis of dynamic systems [35], but their introduction to music domain was done by Foote [6] in 1999 and since then, there have been appearing different techniques for computing this matrices which highlight different aspects of the audio features with which the SSM is formed. The SSM relies on the concept of self-similarity. The self-similarity is measured by a similarity function s which is applied to the audio features representation. As an example [6], the similarity between two feature vectors derived from audio windows y of length N is a function that can be expressed as in Eq. 1. The results is a N -square matrix $SSM \in \mathbb{R}^{N \times N}$ being N the time dimension.

$$SSM(n, m) = s(y_n, y_m) \quad (1)$$

where $n, m \in [1, \dots, N]$.

The similarity function is obtained by the calculation of a distance between the two feature y vectors mentioned before. In the literature, this distance is usually calculated as the Euclidean distance δ_{eucl} or the cosine distance δ_{cos} .

$$\delta_{eucl} = \|u - v\| \quad (2)$$

$$\delta_{cos} = 1 - \frac{u \cdot v}{\|u\| \cdot \|v\|} \quad (3)$$

where u and v are time series vectors.

Self-Similarity Matrices can be computed from different audio features representations such as MFCCs or chromas depending on the properties we need to capture from the music, and they can also be obtained by combining different frame-level audio features [29]. MFCCs are more related to instrumentation and timbre whereas chromas capture better the beat, tempo and rhythmic information. Once the similarity function has been applied to all pairs of vectors of the audio features representation and the SSM has been calculated, we can filter the SSM by applying thresholding techniques, smoothing or invariance transposition so we can increase the paths and emphasize the diagonal information and obtain a more adequate representation of the SSM to visualize and

analyze the representation of the structure. The SSM can also be obtained with other techniques such as clustering methods as Serra et al. proposed in [36], where the SSM is obtained by applying the k - nn algorithm. Then, this matrices can be smoothed or post-processed in order to do a unsupervised clustering classification algorithms as described in section II-A. One example is the work In Serra et al. work [36] the resultant SSM is convolved with a gaussian filter in order to make a clustering of the different parts of musical pieces.

After Foote in 1999 defined the SSM, in 2003, Goto [7] defined a variant of the SSM which is called Self-Similarity Lag Matrix (SSLM). The dimensions of this matrix are not $N \times N$ but $N \times L$, being L the *lag factor*. With this representation it is possible to plot the relations between past events and their repetitions in the future. The SSLM is a non-square matrix: $SSLM \in \mathbb{R}^{N \times L}$. Some libraries calculate this SSLM after computing the SSM or the recurrence plot as in Eq. 4.

$$SSLM(i, j) = SSM_{k+1, j} \quad (4)$$

with $i, j = 1, \dots, N$ and $k = i + j - 2 \pmod{N}$.

The choice of the type of audio features representation for computing the SSMs or SSLMs, and the choice of using SSMs or SSLMs is one of the most important steps when solving a MIR task that has to be studied depending on the issue we want to face.

D. Datasets

Previous works had been tested in the annual Music Information Retrieval Evaluation eXchange (MIREX [37]). MIREX is a framework for evaluating music information retrieval algorithms. The evaluation tasks are defined by the research community under the coordination of International Music Information Retrieval Systems Evaluation Laboratory at the University of Illinois at Urbana Champaign [38]. MIREX's testing databases collections contains MIREX09, MIREX10 and then MIREX12 datasets.

The first dataset of MIREX campaign structure segmentation task was the MIREX09 dataset consisting of Beatles songs plus another smaller dataset⁴. Beatles dataset have 2 annotation versions, one is Paulus Beatles or Beatles-TUT⁵ dataset and the second one is the Isophonic Beatles or Beatles-ISO⁶ dataset. The second MIREX dataset was MIREX10, formed by RWC [39] dataset. This dataset has 2 annotation versions; RWC-A⁷ of QUAERO project which is the one

⁴<http://ifs.tuwien.ac.at/mir/audiosegmentation.html>

⁵http://www.cs.tut.fi/sgn/arg/paulus/beatles_sections_TUT.zip

⁶<http://isophonics.net/content/reference-annotations>

⁷<http://musicdata.gforge.inria.fr>

which corresponds to MIREX10 and RWC-B⁸ [40], which is the original annotated version which the annotation guidelines were established by [41].

A few years later, the MIREX12 dataset provided a greater variety of songs than the MIREX10 [42]. MIREX12 is a dataset formed by the "Structural Analysis of Large Amounts of Music Information" (SALAMI⁹) dataset which has evolved in its more recent version, the SALAMI 2.0 database. The analysis of MIREX structure segmentation task was published in 2012 [43]. Our work uses the available SALAMI 2.0 dataset.

III. AUDIO PROCESSING

This work is based on the previous works of Schuler, Grill et al. [3], [4], who explain the procedure of how to obtain the SSLMs from MFCCs features. We will extend these works by calculating the SSLMs from chroma features and applying also the euclidean distance in order to give a comparison and provide the best-performing input to the NN model.

A. Mel Spectrogram

The first step to process the audio files to extract their different features is to compute the Short-Time-Fourier-Transform (STFT) with a Hanning window of 46ms (2048 samples at 44.1kHz sample rate) and an overlap of 50%. Then, a mel-scaled filterbank of 80 triangular filters from 80Hz to 16kHz and the amplitudes magnitudes are scaled logarithmically to obtain the mel-spectrogram (MLS) of the audio file. We have used the *librosa library* [44] so, the mel-spectrogram can be computed directly giving these parameters. The MLS will be max-pooled by a factor of $p = 6$ to give the Neural Network a manageable size input. The size of the MLS matrix is $[P, N]$ with P being the number of frequency bins (that are equal to the number of triangular filters) and N the number of time frames. We name each MLS frame \mathbf{x}_i with $i = 1 \dots N$.

B. Self-Similarity Lag Matrix from MFCCs

The method that we used to generate the SSLMs¹⁰ is the same method that Grill and Schluter used in [4] and [5], which in turn derives from Serrá et al. [45].

The first step after computing each frame mel-spectrogram \mathbf{x}_i is to pad a vector Φ_i with a white noise constant value of -70dB of L lag seconds in the time dimension and P mel-bands in the frequency dimension, at the beginning of the mel-spectrogram.

$$\tilde{\mathbf{x}}_i = \Phi_i \parallel \mathbf{x}_i \quad (5)$$

where vector Φ_i is a vector of shape $[L, P]$.

Then, a max-pool of a factor of p_1 is done in the time dimension as shown in Eq. 6.

$$\mathbf{x}'_i = \max_{j=1 \dots p_1} (\tilde{\mathbf{x}}_{(i-1)p_1+j}) \quad (6)$$

After that, we apply a Discrete Cosine Transform of Type II of each frame omitting the first element.

$$\tilde{\mathbf{X}}_i = \text{DCT}_{2 \dots P}^{(\text{II})}(\mathbf{x}'_i) \quad (7)$$

where P are the number of mel-bands.

Now we stack the time frames by a factor m so we obtain the time series in Eq. 8. The resulting $\hat{\mathbf{X}}_i$ vector has dimensions $[(P-1)*m, (N+L)/p_1]$ where N is the number of time frames before the max-pooling and L the lag factor in frames.

$$\hat{\mathbf{X}}_i = [\tilde{\mathbf{X}}_i^T \parallel \tilde{\mathbf{X}}_{i+m}^T]^T \quad (8)$$

The final SSLM matrix is obtained by calculating a distance between the vectors $\hat{\mathbf{X}}_i$. Two different distance metrics have been implemented: euclidean and cosine distance. This will allow us to make a comparison between them and deduce the SSLM that will perform better.

Then, the distance between two vectors $\hat{\mathbf{X}}_i$ and $\hat{\mathbf{X}}_{i-l}$ using the distance metric δ is

$$D_{i,l} = \delta(\hat{\mathbf{X}}_i, \hat{\mathbf{X}}_{i-l}), \quad l = 1 \dots \left\lfloor \frac{L}{p} \right\rfloor \quad (9)$$

where δ is the distance metric as defined in Eqs. 2 and 3.

Then, we compute an equalization factor $\varepsilon_{i,l}$ with a quantile κ of the distances $\delta(\hat{\mathbf{X}}_i, \hat{\mathbf{X}}_{i-j})$ and for $j = 1 \dots \left\lfloor \frac{L}{p} \right\rfloor$

$$\varepsilon_{i,l} = Q_\kappa \left(D_{i,l}, \dots, D_{i, \left\lfloor \frac{L}{p} \right\rfloor} \parallel D_{i-l,1}, \dots, D_{i-l, \left\lfloor \frac{L}{p} \right\rfloor} \right) \quad (10)$$

We now remove L/p lag bins in the time dimension at the beginning of the distances vector $D_{i,l}$ and in the equalization factor vector $\varepsilon_{i,l}$, and we apply Eq. 6 with max-pooling factor p_2 . Finally we obtain the SSLM applying Eq. 11.

$$R_{i,l} = \sigma \left(1 - \frac{D_{i,l}}{\varepsilon_{i,l}} \right) \quad (11)$$

where $\sigma(x) = \frac{1}{1+e^{-x}}$

Once the SSLM has been obtained, we pad $\gamma = 50$ time frames of pink noise at the beginning and end of the SSLM and MLS matrices and we normalized each frequency band to zero mean and unit variance for MLS and each lag band for SSLMs. Note also that if there are some time frames that have the same values, the cosine distance would give a NAN (not-a-number) value. We avoid this by converting all this NAN values into zero as the last step of the SSLM computation.

C. Self-Similarity Lag Matrix from Chromas

The process of computing the SSLM from chroma features is similar to the method explained in section III-B. The difference here is that instead of starting with padding the mel-spectrogram in Eq. 5, we pad the STFT. After applying the max-pooling in Eq. 6, we compute the chroma filters instead of computing the DCT in Eq. 7. The rest of the process is the same as described in section III-B.

All the values of the parameters used in obtaining the Self-Similarity Matrices are summarized in Table III. In addition to the euclidean and cosine metrics, and MFCCs and chromas

⁸<http://staff.aist.go.jp/m.goto/RWC-MDB/AIST-Annotation>

⁹<https://ddmal.music.mcgill.ca/research/SALAMI/>

¹⁰<https://github.com/carlosholivan/SelfSimilarityMatrices>

audio features, we will compare two pooling strategies. The first one is to make a max-pooling of factor $p = 6$ described in Eq. 6 of the STFT and mel-spectrogram for SSLMs from chromas and MFCCs, respectively. The other pooling strategy is the one showed in Fig. 2. We denote this pooling variants as 6_{pool} and $2_{\text{pool}13}$. The total time for processing all the SSLMs (MFCCs and cosine distance) was a factor of 4 faster for 6_{pool} than $2_{\text{pool}13}$.

The general schema of the pre-processing block is depicted in Fig. 2.

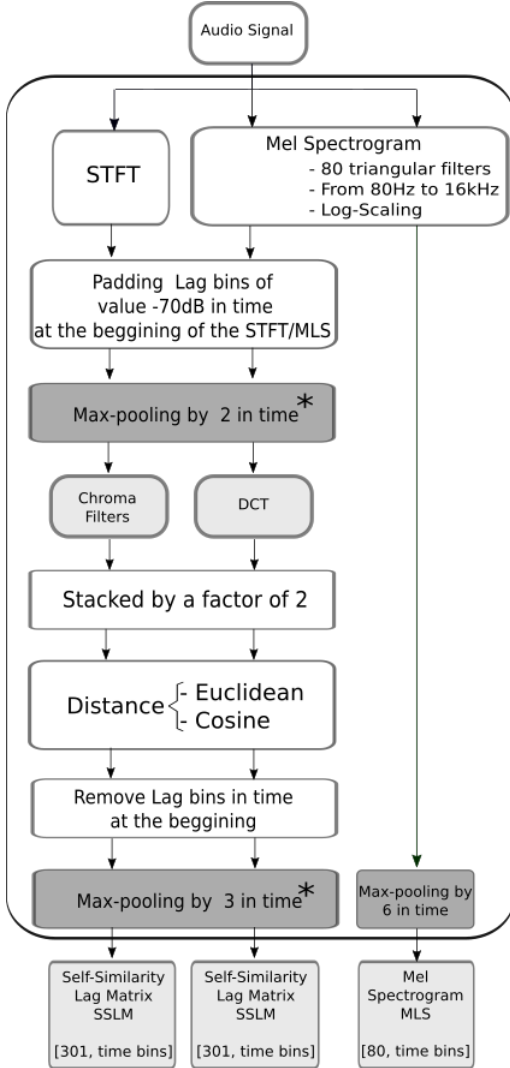


Fig. 2: General block diagram of the pre-processing block in Fig. 1. The * mark in max-pooling blocks refers to the 2 variants done in this work, one is the $2_{\text{pool}13}$ which is the one showed in the scheme and the other one, 6_{pool} is computed by applying the max-pooling of factor 6 in the first * block and removing the second * block of the scheme.

IV. DATASET

The algorithm was trained, validated and tested on a subset of the Structural Analysis of Large Amounts of Music Information (SALAMI) dataset [46]. SALAMI dataset contains 1048 double annotated pieces from which we could obtain

TABLE III: Parameter final values.

Parameter	Symbol	Value	Units
sampling rate	sr	44100	Hz
window size	w	46	ms
overlap	-	50	%
hop length	h	23	ms
lag	L	14	s
pooling factor 6_{pool}	p	6	-
$2_{\text{pool}13}$	$p1$	2	-
	$p2$	3	-
stacking parameter	m	2	-
quantile	κ	0.1	-
final padding	γ	50	frames

1006 pieces. For the training of the model we used the text file of labels from annotator 1 and for the songs that were not annotated by annotator 1, we use the same text file but from annotator 2.

There is important to highlight that, as described in [22], previous works such as [3], [4] and [5] use a private non-accessible dataset of 733 songs from which 633 pieces were using for training and 100 for validation. Therefore, we re-implemented the work presented in [4] but we ran it in our dataset composed by only SALAMI pieces and annotations. We split our 1006 SALAMI audio tracks into 65%, 15% and 20%, resulting in 650, 150 and 206 pieces for training, validation and testing respectively.

A. Labelling Process

As [3] explained, it is necessary to transform the labels of SALAMI text files into Gaussian functions so that the Neural Network can be trained correctly. We first set the mean values of the Gaussian functions by transforming the labels in seconds in time frames as showed in Eq. 12 constructing vector μ_i of dimension equal to the number of labels in the text file. In Eq. 12, $label_i$ are the labels in seconds extracted from SALAMI text file "functions", $p1, p2, h, sr$ and γ are defined in Table III.

$$\mu_i = \frac{label_i}{p1 * p2} + \frac{h * sr}{\gamma} \quad (12)$$

Then we transform this labels in seconds into frames by applying a gaussian function with standard deviation $\sigma = 0.1$ and μ_i equal to each label value in Eq. 12. In Eq. 13 the labels are in seconds, so in this equation, a mean equal to 1 is set where a label with a standard deviation σ is found for each time frame position y'_i .

$$gaussian_labels_i = g(y'_i, \mu_i, \sigma) \quad (13)$$

with

$$g(x, \mu, \sigma) = \frac{1}{\sqrt{2\pi}\sigma} e^{-\frac{1}{2}\left(\frac{x-\mu}{\sigma}\right)^2}$$

where y'_i is a vector of $\frac{y_i * \gamma + \frac{w}{2}}{sr}$ frames from $i = 1 \dots \lfloor \frac{N}{p1 p2} \rfloor$.

To train the model, we removed the first tag from each text file due to the proximity of the first two tags in almost all files and the uselessness of the Neural Network identifying the beginning of the file. It is also worth mentioning the fact

that we have resampled all the songs in the SALAMI database at a single *sampling rate* of 44100Hz as showed in Table III.

V. MODEL

The model developed in this work for boundary detection is showed in Fig. 3. Once the matrices of the preprocessing step are obtained they are padded and normalized to form the input of a Convolutional Neural Network (CNN). The obtained predictions are post-processed with a peak-picking and threshold algorithm to obtain the final predictions.

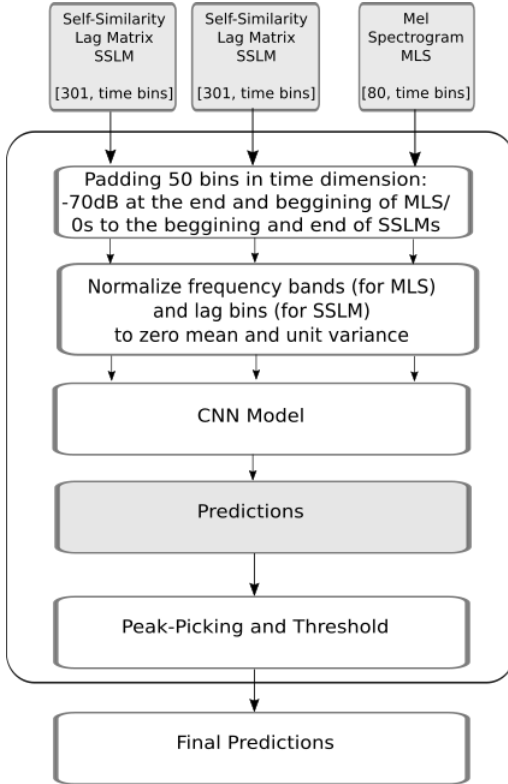


Fig. 3: General block diagram of the Neural Network block in Fig. 1.

A. Convolutional Neural Network

The model proposed in this paper is nearly the same that the model proposed in [3] and [4], so we could compare the results and make a comparison with different input strategies as Cohen [22] did.

The model is composed by a CNN whose relevant parameters are showed in Table IV. The difference between this model and the model proposed in [3] and [4] is that our final two layers are not dense layers but convolutional layers in one dimension because we do not crop the inputs and get a single probability value at the output, but we give the Neural Network the whole matrix (so we use a batch size of 1 for training) and we obtain a time prediction curve at the output. The general schema of the CNN is showed in Fig. 4.

TABLE IV: CNN architecture parameters of the schema presented in Fig. 4

Layer	Parameters
Convolution 1 + Leaky ReLU	output feature maps: 32 kernel size: 5 x 7 stride: 1 x 1 padding: (5-1)/2 x (7-1)/2
Max-Pooling	kernel size: 5 x 3 stride: 5 x 1 padding: 1 x 1
Convolution 2 + Leaky ReLU	output feature maps: 64 kernel size: 3 x 5 stride: 1 x 1 padding: (3-1)/2 x (5-1)*3/2 dilation: 1 x 3
Convolution 3 + Leaky ReLU	output feature maps: 128 kernel size: 1 x 1 stride: 1 x 1 padding: 0 x 0
Convolution 4	output feature maps: 1 kernel size: 1 x 1 stride: 1 x 1 padding: 0 x 0

B. Training Parameters

We trained our CNN with *Binary Cross Entropy* or BCE-withLogitsLoss in Pytorch [47] as the loss function which includes a sigmoid activation function at the end of the Neural Network, a *learning rate* of 0.001 and Adam optimizer [48]. We used batches of size 1 because we provide the network with songs of different duration as a whole. The models were trained on a GTX 980 Ti Nvidia GPU and we used TensorboardX [49] to graph the loss and F-score of training and validation in real time.

C. Peak-Picking

Peak-picking consists on selecting the peaks of the output signal of the CNN that will be identified as boundaries of the different parts of the song. Each boundary on the output signal is considered true when no other boundary is detected within 6 seconds. The application of a threshold help us to discriminate boundaries values that are not higher than an optimum threshold that has been determined by testing the pieces for each threshold value belonging to [0, 1]. The optimum threshold is the one for which the F-score is higher. When training different inputs the threshold may vary. We set a threshold of 0.205 for only MLS input as it is showed in Fig. 5 and for the rest of our input variants is showed in Table VI. From the optimum threshold calculation, we can observe that almost all optimum threshold values for each input variant belong to [2.05, 2.6] Fig. 5 shows Recall, Precision and F-score values (see Section ?? of the testing dataset evaluated for each possible threshold value. Note that the Precision curve should increase till it reaches a threshold of value equal to 1, but as the peaks of our output signals does not reach this value we can observe a decrease of the threshold value when it exceeds 0.7.

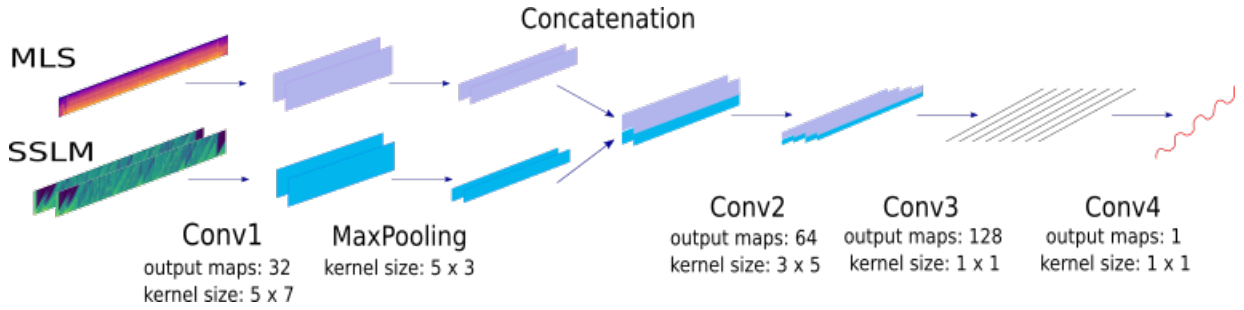


Fig. 4: Schema of the Convolutional Neural Network implemented. The main parameters are presented in Table IV.

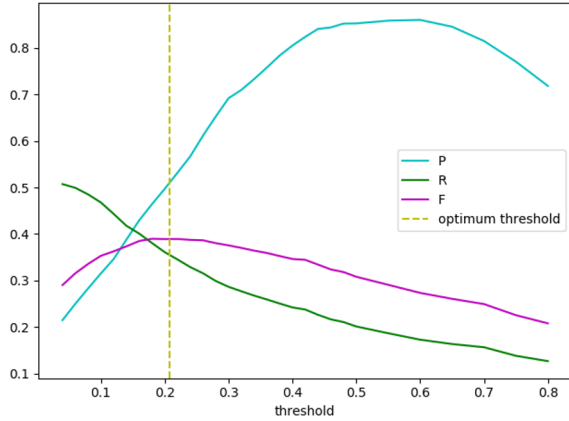


Fig. 5: Threshold calculation through MLS test after 180 epochs of training only MLS.

VI. EXPERIMENTS AND RESULTS

A. Evaluation Metrics

MIREX’s campaigns uses two evaluation measures which are *Median Deviation* and *Hit Rate*. The *Hit Rate* (also called F-score or F-measure) is denoted by F_β , where $\beta = 1$ is the most frequently measure used in previous works. Nieto et al. [50] set a value of $\beta = 0.58$, but the truth is that F_1 is the most used metric in MIREX works. We will later give our results for both β values. The *Hit Rate* score F_1 is normally evaluated for $\pm 0.5s$ and $\pm 3s$ time-window tolerances, but in recent works most of the results are given only for $\pm 0.5s$ tolerance which is the most restrictive one. We test our model with MIREX algorithm [51] which give us the Precision, Recall and F-measure parameters.

$$\text{Precision : } P = \frac{TP}{TP + FP} \quad (14)$$

$$\text{Recall : } R = \frac{TP}{TP + FN} \quad (15)$$

$$\text{F measure : } F_\beta = (1 + \beta^2) \frac{P \cdot R}{\beta^2 \cdot P + R} \quad (16)$$

Where:

- TP: True Positives. Estimated events of a given class that start and end at the same temporal positions as reference

events of the same class, taking into account a tolerance time-window.

- FP: False Positives. Estimated events of given class that start and end at temporal positions where no reference events of the same class does, taking into account a tolerance time-window.
- FN: False Negatives. Reference events of a given class that start and end at temporal positions where no estimated events of the same class does, taking into account a tolerance time-window.

B. Results

TABLE V: Results of boundaries estimation according to different pooling strategies, distances and audio features for $\pm 0.5s$ and a threshold of 0.205.

Tolerance: $\pm 0.5s$ and Threshold: 0.205					
	Input	Epochs	P	R	F_1
6pool	MLS	180	0.501	0.359	0.389
	SSLM ^{MFCCs} _{euclidean}	180	0.472	0.318	0.361
	SSLM ^{MFCCs} _{cosine}	180	0.477	0.311	0.355
	SSLM ^{chromas} _{euclidean}	180	0.560	0.228	0.297
	SSLM ^{chromas} _{cosine}	180	0.508	0.254	0.312
2pool3	SSLM ^{MFCCs} _{euclidean}	120	0.422	0.369	0.375
	SSLM ^{MFCCs} _{cosine}	120	0.418	0.354	0.366
Previous works					
2pool3	MLS [3]	-	0.555	0.458	0.465
	SSLM ^{MFCCs} _{cosine} [4]	-	-	-	0.430

1) *Pooling Strategy*: We first train the Neural Network with each input matrix (see Fig. 3) separately in order to know what input performs better. We train MLS and SSLMs obtained from MFCCs and Chromas and applying euclidean and cosine distances, and we also give the results for both of the pooling strategies mentioned before, 6pool (lower resolution) and 2pool3 (higher resolution). As mentioned in section IV, we removed the first label of the SALAMI text files corresponding to 0.0s label. Results in terms of F score, Precision and Recall are showed in Table V. Note that the results showed from previous works used a different threshold value.

In Fig. 6 we show an example of the boundaries detection results for some of our input variants on the MLS and SSLMs.

TABLE VI: Results of boundary estimation with tolerance $\pm 0.5s$ and optimum threshold in terms of F-score, Precision and Recall. Note that results from previous works did not use the same threshold value.

Tolerance: $\pm 0.5s$ with 2pool3 matrices							
Input	Train Database	Epochs	Thresh.	P	R	F ₁ (std)	F _{0.5s}
MLS + SSLM _{euclidean} ^{MFCCs}	SALAMI	140	0.24	0.441	0.415	0.402 (0.163)	0.414
MLS + SSLM _{cosine} ^{MFCCs}	SALAMI	140	0.24	0.428	0.407	0.396 (0.158)	0.404
MLS + (SSLM _{euclidean} ^{MFCCs} + SSLM _{euclidean} ^{chromas})	SALAMI	100	0.24	0.465	0.400	0.407 (0.160)	0.419
MLS + (SSLM _{cosine} ^{MFCCs} + SSLM _{cosine} ^{chromas})	SALAMI	100	0.24	0.444	0.416	0.404 (0.166)	0.417
MLS + (SSLM _{euclidean} ^{MFCCs} + SSLM _{cosine} ^{MFCCs})	SALAMI	100	0.24	0.445	0.421	0.409 (0.173)	0.416
MLS + (SSLM _{euclidean} ^{chromas} + SSLM _{cosine} ^{chromas})	SALAMI	100	0.24	0.457	0.396	0.400 (0.157)	0.420
MLS + (SSLM _{euclidean} ^{chromas} + SSLM _{cosine} ^{chromas} + SSLM _{euclidean} ^{MFCCs} + SSLM _{cosine} ^{MFCCs})	SALAMI	100	0.26	0.526	0.374	0.411 (0.169)	0.451
Supervised Neural Networks previous works							
MLS + SSLM _{cosine} ^{MFCCs} [4] (2015)	Private	-		0.646	0.484	0.523	0.596
MLS + SSLM _{cosine} ^{MFCCs} [22] (2017)	SALAMI	-		0.279	0.300	0.273 (0.132)	-
MLS + (SSLM _{cosine} ^{MFCCs} + SSLM _{cosine} ^{chromas}) [22] (2017)	SALAMI	-		0.470	0.225	0.291 (0.120)	-

We obtained lower results than [4] but higher results than [22] who tried to re-implement [4]. The reasons for this difference could be that the database used by Grill and Schluter [4] to train their model, had 733 non-public pieces.

Cohen and Peeters [22], as in our work, trained their model only with pieces from the SALAMI database, so that our results can be compared with theirs, since we trained, validated and tested our Neuronal Network with the same database (although they had 732 SALAMI pieces and we had 1006).

In view of the results in Table V, we can affirm that doing a max-pooling of 2, then computing the SSLMs and doing another max-pooling of 3 afterwards increment the results but not too much. This procedure not only takes much more time to compute the SSLMs but also the training takes also much more time and it does not perform better results in terms of F-score.

2) *Inputs Combination:* With the higher results in Table V we make a combination of them as in [4] and later in [22]. A summary of our results can be found in Table VI.

The inputs combination that performs the best in [22] was MLS + (SSLM_{cosine}^{MFCCs} + SSLM_{cosine}^{chromas}) for which $F_1 = 0.291$. We overcome that result for the same combination of inputs obtaining $F_1 = 0.404$. In spite of that, and the statement in [4] which says that cosine distance performs better than the euclidean one, we found that the best-performing inputs combination is MLS + (SSLM_{euclidean}^{chromas} + SSLM_{cosine}^{chromas} + SSLM_{euclidean}^{MFCCs} + SSLM_{cosine}^{MFCCs}) for which $F_1 = 0.411$. There is not a huge improvement in the F-measure but it is still our best result.

VII. CONCLUSIONS

In this work we have developed a comparative study to set the best-performing way to compute the inputs of a Convolutional Neural Network to identify boundaries in music pieces by combining diverse methods of generating the SSLMs. We demonstrate that by computing a max-pooling of factor 6 at the beginning of the process not only takes much less time but

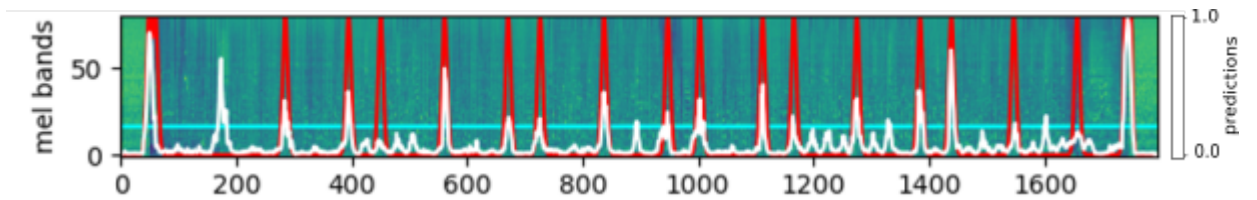
also the training of the Neural Network is faster and it does not affect the results as much as it could be thought. We also give the best-performance combination of inputs of SSLMs outperforming the results given in [22]. Despite the fact that we could not obtain [3] and [4] results with nearly the same model, we outperform the results in [22] who also tried to re-implement the model described in the previous literature. There has to be highlighted the fact that [3] and [4] had at their disposition a private dataset of 733 pieces that they used for training the model, and in this paper the model has been trained only with the public available dataset of SALAMI 2.0, so our results are maybe lower because of that, but our results outperform other works that also trained their models with only the public available SALAMI 2.0 database.

As commented, the results obtained in this work improve those presented previously, if the database used is the same. However, the accuracy in obtaining the boundaries in musical pieces is relatively low and, to some extent, difficult to use. This makes it necessary, on the one hand, to continue studying different methods that allow a correct structural analysis of music and, on the other hand, to obtain databases that are properly labeled and contain a high number of musical pieces.

In any case, the results obtained are promising and allow us to adequately set out the bases for future work.

REFERENCES

- [1] N. Cook, *A guide to musical analysis*. Oxford University Press, USA, 1994.
- [2] M. Müller, *Fundamentals of music processing: Audio, analysis, algorithms, applications*. Springer, 2015.
- [3] K. Ullrich, J. Schlüter, and T. Grill, "Boundary detection in music structure analysis using convolutional neural networks.," in *ISMIR*, pp. 417–422, 2014.
- [4] T. Grill and J. Schlüter, "Music boundary detection using neural networks on spectrograms and self-similarity lag matrices.," in *2015 23rd European Signal Processing Conference (EUSIPCO)*, pp. 1296–1300, IEEE, 2015.
- [5] T. Grill and J. Schlüter, "Music boundary detection using neural networks on combined features and two-level annotations.," in *ISMIR*, pp. 531–537, 2015.



(a) CNN predictions on MLS

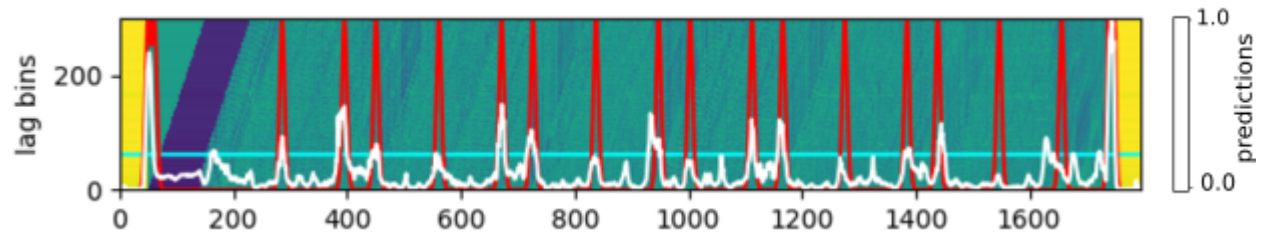
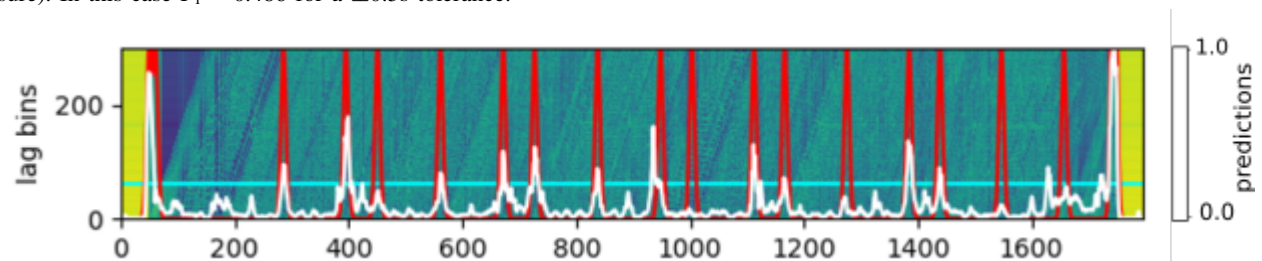
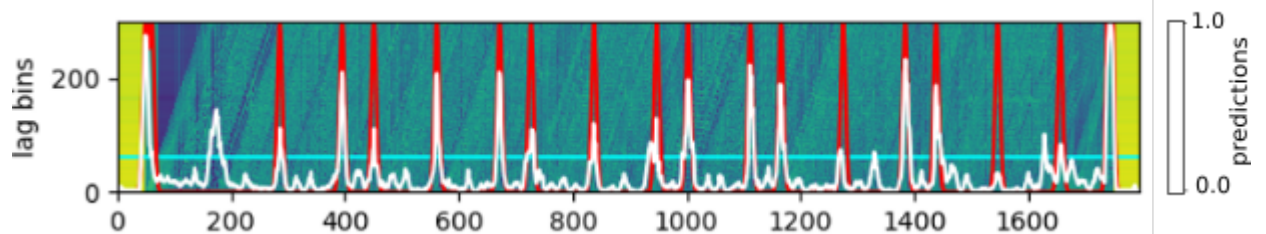
(b) CNN predictions on SSLM calculated with MFCCs and euclidean distance with 2pool3 (best-performance SSLM input in terms of F-measure). In this case $F_1 = 0.486$ for a $\pm 0.5s$ tolerance.(c) CNN predictions on SSLM calculated with MFCCs and cosine distance with 2pool3. In this case $F_1 = 0.686$ for a $\pm 0.5s$ tolerance.(d) CNN predictions on SSLM from MFCCs with cosine distance for model $MLS + (SSLM_{euclidean}^{MFCCs} + SSLM_{cosine}^{MFCCs})$. In this case $F_1 = 0.75$ for a $\pm 0.5s$ tolerance.

Fig. 6: Boundaries predictions using CNN on different inputs obtained from the "Live at LaBoca on 2007-09-28" of DayDrug corresponding to the 1358 song of SALAMI 2.0 database. The ground truth from SALAMI annotations are the gaussians in red, the model predictions is the white curve and the threshold is the horizontal yellow line. Note that the prediction have been rescaled in order to plot them on the MLS and SSLMs images. All these images have been padded according to what is explained in the previous paragraphs and then normalized to zero mean and unit variance.

- [6] J. Foote, "Visualizing music and audio using self-similarity," in *Proceedings of the seventh ACM international conference on Multimedia (Part 1)*, pp. 77–80, 1999.
- [7] M. Goto, "A chorus-section detecting method for musical audio signals," in *2003 IEEE International Conference on Acoustics, Speech, and Signal Processing, 2003. Proceedings. (ICASSP'03)*, vol. 5, pp. V–437, IEEE, 2003.
- [8] T. Zhang and C.-C. J. Kuo, "Heuristic approach for generic audio data segmentation and annotation," in *Proceedings of the seventh ACM international conference on Multimedia (Part 1)*, pp. 67–76, 1999.
- [9] J. Paulus and A. Klapuri, "Music structure analysis with a probabilistic fitness function in MIREX2009," in *Proc. of the Fifth Annual Music Information Retrieval Evaluation eXchange*, (Kobe, Japan), Oct 2009. Extended abstract.
- [10] M. Mauch, K. C. Noland, and S. Dixon, "Using musical structure to enhance automatic chord transcription.," in *ISMIR*, pp. 231–236, 2009.
- [11] G. Sargent, S. A. Raczynski, F. Bimbot, E. Vincent, and S. Sagayama, "A music structure inference algorithm based on symbolic data analysis." MIREX - ISMIR 2011, Oct. 2011. Poster.
- [12] F. Kaiser, T. Sikora, and G. Peeters, "Mirex 2012-music structural segmentation task: Ircamstructure submission," *Proceedings of the Music Information Retrieval Evaluation eXchange (MIREX)*, 2012.
- [13] B. McFee and D. Ellis, "Dp1, mp1, mp2 entries for mirex 2013 structural segmentation and beat tracking," *Proceedings of the Music Information Retrieval Evaluation eXchange (MIREX)*, 2013.
- [14] O. Nieto and J. P. Bello, "Mirex 2014 entry: 2d fourier magnitude coefficients," *Proceedings of the Music Information Retrieval Evaluation eXchange (MIREX)*, 2014.
- [15] C. Cannam, E. Benetos, M. Mauch, M. E. Davies, S. Dixon, C. Landone, K. Noland, and D. Stowell, "Mirex 2015: Vamp plugins from the centre for digital music," *Proceedings of the Music Information Retrieval Evaluation eXchange (MIREX)*, 2015.
- [16] O. Nieto, "Mirex: Msaf v0. 1.0 submission," 2016.
- [17] J. Schlüter, K. Ullrich, and T. Grill, "Structural segmentation with

- convolutional neural networks mirex submission,” *Tenth running of the Music Information Retrieval Evaluation eXchange (MIREX 2014)*, 2014.
- [18] T. Grill and J. Schlüter, “Structural segmentation with convolutional neural networks mirex submission,” *Proceedings of the Music Information Retrieval Evaluation eXchange (MIREX)*, p. 3, 2015.
- [19] D. Turnbull, G. R. Lanckriet, E. Pampalk, and M. Goto, “A supervised approach for detecting boundaries in music using difference features and boosting,” in *ISMIR*, pp. 51–54, 2007.
- [20] G. Sargent, F. Bimbot, and E. Vincent, “A regularity-constrained viterbi algorithm and its application to the structural segmentation of songs,” 2011.
- [21] J. Schlüter and S. Böck, “Improved musical onset detection with convolutional neural networks,” in *2014 IEEE International Conference on Acoustics, Speech and Signal Processing (ICASSP)*, pp. 6979–6983, IEEE, 2014.
- [22] A. Cohen-Hadria and G. Peeters, “Music structure boundaries estimation using multiple self-similarity matrices as input depth of convolutional neural networks,” in *Audio Engineering Society Conference: 2017 AES International Conference on Semantic Audio*, Audio Engineering Society, 2017.
- [23] J. Paulus, M. Müller, and A. Klapuri, “State of the art report: Audio-based music structure analysis,” in *ISMIR*, pp. 625–636, Utrecht, 2010.
- [24] J. Foote, “Automatic audio segmentation using a measure of audio novelty,” in *2000 IEEE International Conference on Multimedia and Expo. ICME2000. Proceedings. Latest Advances in the Fast Changing World of Multimedia (Cat. No. 00TH8532)*, vol. 1, pp. 452–455, IEEE, 2000.
- [25] F. Kaiser and G. Peeters, “Multiple hypotheses at multiple scales for audio novelty computation within music,” in *2013 IEEE International Conference on Acoustics, Speech and Signal Processing*, pp. 231–235, IEEE, 2013.
- [26] B. Logan and S. Chu, “Music summarization using key phrases,” in *2000 IEEE International Conference on Acoustics, Speech, and Signal Processing. Proceedings (Cat. No. 00CH37100)*, vol. 2, pp. II749–II752, IEEE, 2000.
- [27] J.-J. Aucouturier and S. Mark, “Segmentation of musical signals using hidden markov models,” in *In Proc. 110th Convention of the Audio Engineering Society*, Citeseer, 2001.
- [28] M. Levy and M. Sandler, “Structural segmentation of musical audio by constrained clustering,” *IEEE transactions on audio, speech, and language processing*, vol. 16, no. 2, pp. 318–326, 2008.
- [29] C. J. Tralie and B. McFee, “Enhanced hierarchical music structure annotations via feature level similarity fusion,” in *ICASSP 2019-2019 IEEE International Conference on Acoustics, Speech and Signal Processing (ICASSP)*, pp. 201–205, IEEE, 2019.
- [30] B. McFee and J. P. Bello, “Structured training for large-vocabulary chord recognition,” in *ISMIR*, pp. 188–194, 2017.
- [31] L. Lu, M. Wang, and H.-J. Zhang, “Repeating pattern discovery and structure analysis from acoustic music data,” in *Proceedings of the 6th ACM SIGMM international workshop on Multimedia information retrieval*, pp. 275–282, 2004.
- [32] J. Paulus and A. Klapuri, “Music structure analysis by finding repeated parts,” in *Proceedings of the 1st ACM workshop on Audio and music computing multimedia*, pp. 59–68, 2006.
- [33] M. C. McCallum, “Unsupervised learning of deep features for music segmentation,” in *ICASSP 2019-2019 IEEE International Conference on Acoustics, Speech and Signal Processing (ICASSP)*, pp. 346–350, IEEE, 2019.
- [34] S. Dieleman and B. Schrauwen, “End-to-end learning for music audio,” in *2014 IEEE International Conference on Acoustics, Speech and Signal Processing (ICASSP)*, pp. 6964–6968, IEEE, 2014.
- [35] E. Jp, “Recurrence plots of dynamical systems,” *Europhysics Letters*, vol. 5, pp. 973–977, 1987.
- [36] J. Serra, M. Müller, P. Grosche, and J. L. Arcos, “Unsupervised music structure annotation by time series structure features and segment similarity,” *IEEE Transactions on Multimedia*, vol. 16, no. 5, pp. 1229–1240, 2014.
- [37] J. S. Downie, A. F. Ehmann, M. Bay, and M. C. Jones, “The music information retrieval evaluation exchange: Some observations and insights,” in *Advances in music information retrieval*, pp. 93–115, Springer, 2010.
- [38] J. S. Downie, “The music information retrieval evaluation exchange (2005–2007): A window into music information retrieval research,” *Acoustical Science and Technology*, vol. 29, no. 4, pp. 247–255, 2008.
- [39] M. Goto *et al.*, “Development of the rwc music database,” in *Proceedings of the 18th International Congress on Acoustics (ICA 2004)*, vol. 1, pp. 553–556, 2004.
- [40] M. Goto *et al.*, “Aist annotation for the rwc music database,” in *ISMIR*, pp. 359–360, 2006.
- [41] F. Bimbot, E. Deruty, G. Sargent, and E. Vincent, “Methodology and conventions for the latent semiotic annotation of music structure,” 2012.
- [42] A. F. Ehmann, M. Bay, J. S. Downie, I. Fujinaga, and D. De Roure, “Music structure segmentation algorithm evaluation: Expanding on mirex 2010 analyses and datasets,” in *ISMIR*, pp. 561–566, 2011.
- [43] J. B. Smith and E. Chew, “A meta-analysis of the mirex structure segmentation task,” in *Proc. of the 14th International Society for Music Information Retrieval Conference, Curitiba, Brazil*, vol. 16, pp. 45–47, 2013.
- [44] B. McFee, C. Raffel, D. Liang, D. P. Ellis, M. McVicar, E. Battenberg, and O. Nieto, “librosa: Audio and music signal analysis in python,” in *Proceedings of the 14th python in science conference*, vol. 8, 2015.
- [45] J. Serra, M. Müller, P. Grosche, and J. L. Arcos, “Unsupervised detection of music boundaries by time series structure features,” in *Twenty-Sixth AAAI Conference on Artificial Intelligence*, 2012.
- [46] J. B. L. Smith, J. A. Burgoyne, I. Fujinaga, D. De Roure, and J. S. Downie, “Design and creation of a large-scale database of structural annotations,” in *ISMIR*, vol. 11, pp. 555–560, Miami, FL, 2011.
- [47] A. Paszke, S. Gross, S. Chintala, G. Chanan, E. Yang, Z. DeVito, Z. Lin, A. Desmaison, L. Antiga, and A. Lerer, “Automatic differentiation in pytorch,” 2017.
- [48] D. P. Kingma and J. L. Ba, “Adam: A method for stochastic gradient descent,” in *ICLR: International Conference on Learning Representations*, 2015.
- [49] M. Abadi, A. Agarwal, P. Barham, E. Brevdo, Z. Chen, C. Citro, G. S. Corrado, A. Davis, J. Dean, M. Devin, S. Ghemawat, I. Goodfellow, A. Harp, G. Irving, M. Isard, Y. Jia, R. Jozefowicz, L. Kaiser, M. Kudlur, J. Levenberg, D. Mané, R. Monga, S. Moore, D. Murray, C. Olah, M. Schuster, J. Shlens, B. Steiner, I. Sutskever, K. Talwar, P. Tucker, V. Vanhoucke, V. Vasudevan, F. Viégas, O. Vinyals, P. Warden, M. Wattemberg, M. Wicke, Y. Yu, and X. Zheng, “TensorFlow: Large-scale machine learning on heterogeneous systems,” 2015. Software available from tensorflow.org.
- [50] O. Nieto, M. M. Farbood, T. Jehan, and J. P. Bello, “Perceptual analysis of the f-measure for evaluating section boundaries in music,” in *Proceedings of the 15th International Society for Music Information Retrieval Conference (ISMIR 2014)*, pp. 265–270, 2014.
- [51] C. Raffel, B. McFee, E. J. Humphrey, J. Salamon, O. Nieto, D. Liang, D. P. Ellis, and C. C. Raffel, “mir_eval: A transparent implementation of common mir metrics,” in *In Proceedings of the 15th International Society for Music Information Retrieval Conference, ISMIR*, Citeseer, 2014.